Journal of Luminescence 145 (2014) 713–716

Contents lists available at ScienceDirect

Journal of Luminescence

journal homepage: www.elsevier.com/locate/jlumin

Effects of the HfO_2 sinterization temperature on the erbium luminescence

César L. Ordóñez-Romero [a,*], C. Flores J [a], J. Hernández A [a], E. Camarillo G. [a], E. Cabrera B. [a], Manuel Garcia-Hipólito [b], H. Murrieta S. [a]

[a] Instituto de Física, Universidad Nacional Autónoma de México, CU, 04510 México D.F., México
[b] Instituto de Investigación en Materiales, Universidad Nacional Autónoma de México, CU, 04510 México D.F., México

ARTICLE INFO

Article history:
Received 19 February 2013
Received in revised form
21 June 2013
Accepted 23 August 2013
Available online 31 August 2013

Keywords:
Photoluminescence
Excitation
Emission
Hafnium oxide
Erbium

ABSTRACT

The effect of the sinterization temperature of erbium doped hafnium oxide on erbium ion luminescence is studied. Samples were prepared using sinterization temperatures of 400, 600, 800, and 1000 °C over periods of 12 and 24 h. Transitions from the excited states $^4F_{7/2}$ and $^4S_{3/2}$ to the ground state $^4I_{15/2}$ are identified, and this allows for the study of the incorporation of Er^{3+} in the HfO_2 matrix. Results show that the Er^{3+} ions can occupy different sites in the host and the resulting optical behavior depends on the sinterization temperature. The emission efficiency does not depend exclusively on the sinterization temperature but also on the site occupied in the host matrix.

1. Introduction

In recent decades, research efforts on erbium-doped materials have been of great interest for optical communication technology [1,2] and material science. Their strong intra-4f Er^{3+} emission at 1.54 μm, central in fiber optic telecommunications, and their luminescence at higher energies, make them very suitable for a large variety of optoelectronic applications. Previously, most attention was focused on Si-based Er-doped materials and structures [3]. However, it has been found that in most of these materials and structures, optical efficiency cannot present important values due to the low solubility of erbium in silicon and the formation of Auger deexcitation. [4]. Recently, efforts aimed at improving the optical efficiency of Er-doped bulk Si have followed three different lines: (a) the Er solubility improvement in the bulk matrix by codoping techniques [2,3] or by using Er-doped oxides such as Al_2O_3 [5], Y_2O_3 [6], and ZnO [7]; (b) the use of proper sensitizers for Er ions, including nanocrystalline Si (nc-Si) [3,8,9], porous Si [10], and GaN [11], ion sensitizers with a larger cross-section absorption capacity such as Yb [12,13] and Ag [14], and defects in the films [15,16]; and (c) the adoption of optimal sinterization temperatures, which leads to an optimal microstructure environment [17–19]. It is well accepted that within the tendency to miniaturize integrated devices, HfO_2 is one of the most promising high-k dielectric candidates to replace SiO_2 [20]. This is due to its particular capability to provide an ideal host matrix with stable mechanical properties which supply an ideal environment for Er doping with a sufficient amount of oxygen for activating the doped ions. Moreover, the broader band gap of HfO_2 effectively suppresses luminescence thermal quenching effects, enhancing the prospect of HfO_2 as an ideal material for a wide range of optoelectronic applications.

In this work, an approach to improve the luminescence efficiency of Er-doped materials by employing HfO_2 as the host and by finding the optimum sinterization temperature is presented. The experiment was carried out as follows: (1) HfO_2 and erbium-doped HfO_2 (HfO_2:Er) samples were prepared using a very simple chemical technique and temperature treated for equal periods of time and different temperatures, (2) optical absorption of the samples was measured in order to identify the appropriate excitation/emission wavelengths necessary for photoluminescence spectrum measurements, (3) characteristic emission and excitation spectra were obtained for all the sinterization temperatures, and (4) X-ray measurements were performed.

2. Experimental

For the synthesis of HfO_2 powders, typically 12 g of $HfCl_4$ (98% purity, Alfa-Aesar) were dissolved in a solution of 20 ml of deionized water and 20 ml of methanol. The doping with Er was carried out by adding erbium nitrate ($Er(NO_3)_3+6H_2O$, 99.99% purity, Aldrich

* Corresponding author. Tel.: +52 55 56225000x2037.
E-mail address: cloro@fisica.unam.mx (C.L. Ordóñez-Romero).

0022-2313/$ - see front matter © 2013 Elsevier B.V. All rights reserved.
http://dx.doi.org/10.1016/j.jlumin.2013.08.050

Chemical Co.) to the solution. The Er doping concentration was for all cases 1 at%. All reagents were used without any further purification and the mixture was stirred vigorously by using a magnetic stirrer until a homogeneous solution was formed. This solution was then heated to 250 °C and maintained for 20 min until the evaporation of the solvents was complete and a white precipitate was obtained. The precipitate was then completely dried at 350 °C for 10 min at ambient atmosphere and then cooled gradually to room temperature. The dried powders were sintered in air at 400, 600, 800 and 1000 °C for 24 h. Once the HfO_2 and HfO_2:Er (1 at%) powders were temperature treated, 1.2 cm-diameter pellets were made by placing them in a stainless steel die and statically pressed at room temperature at about 100 MPa for 5 min.

In order to identify the absorption wavelengths, a Cary 5000 spectrophotometer was used to obtain the spectra for all the sinterization temperatures of both the doped and undoped samples. The measurements were carried out using standard reflectance scanning with the help of a special fiber optic and an optical circulator. The emission and excitation spectra were measured using a Perkin-Elmer LS 55 fluorescence spectrometer. The chemical composition of the films was measured by energy dispersive spectroscopy (EDS) using an Oxford Pentafet Si–Li detector integrated on a Leica-Cambridge Scanning Electron Microscope model stereoscan 440 (SEM) and the crystalline structure was analyzed by means of X-ray diffraction (XRD) using a Siemens D-5000 difractometer with Cu-Kα radiation.

3. Results and discussion

As mentioned above, the characterization of the samples started with the measurement of the absorption spectra for all the sinterization temperatures and treatment periods. Fig. 1 shows the absorption spectra for the Er-doped (lower curve) and the undoped (upper curve) HfO_2 samples that were temperature treated for 12 h at 800 °C at ambient atmosphere. The HfO_2:Er^{3+} 1% absorption spectrum is labeled with the typical energy levels for the Er ion and the respective excitation wavelengths.

The peaks shown in the lower curve, Fig. 1, are clearly due to the introduction of the erbium ion in the HfO_2 matrix and their positions in the spectrum correspond nicely to the energy levels shown by the free Er ion [21]. From Fig. 1, it is possible to observe that the strongest absorptions take place at the energy levels $^4G_{11/2}$ $^4F_{7/2}$, $^2H_{11/2}$, $^4S_{3/2}$, and $^4F_{9/2}$ that correspond to 379 nm, 491 nm, 520 nm, 549 nm and 650 nm respectively. Once the introduction of the Er into the matrix was confirmed and the energy levels identified and labeled, the chemical characterization was performed. The X-ray diffraction measurements of the samples as a function of the sinterization temperature are shown in Fig. 2. The diffraction curves correspond to the HfO_2:Er samples treated for temperatures 400, 600, 800, and 1000 °C for periods of 12 h.

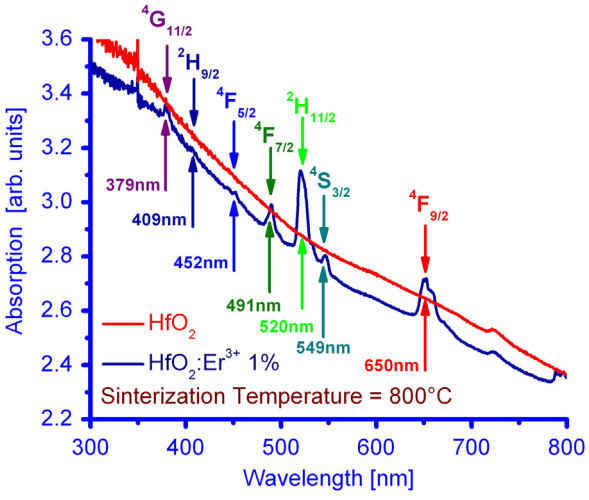

Fig. 1. Absorption spectrum for the 1 at% Er^{3+} doped and un-doped HfO_2 samples sinterized at 800 °C for 12 h.

From the XRD graphs shown in Fig. 2 it is possible to observe that the samples treated at sinterization temperatures below 600 °C present a non-crystalline structure. At higher temperatures, the crystalline formation is evident and it improves as the temperature increases. The distribution peaks in the XRD graphs can be associated nicely with the monoclinic structure of the HfO_2 (JCPDS 43-1017). The diffraction patterns show reflections centered at values of 2θ of 28.3°, 31.6°, 34.3°, 34.6° and 35.4°. These values correspond to the diffracting planes $(\bar{1}\,1\,1)$, (1 1 1), (0 0 2), (0 2 0) and (2 0 0), where the strongest reflection is related to the plane $(\bar{1}\,1\,1)$ associated to the monoclinic structure.

From Fig. 2, in addition to information related to the crystalline structure, it is possible to obtain the size of the crystals for all the sinterization temperatures using the Scherrer formula. The estimated sizes of the crystals were: 15 nm for 400 °C, 20 nm for 600 °C, 28 nm for 800 °C, and 37 nm for 1000 °C. All the estimations were calculated based on the strongest diffraction peak located at 28.3°. Table 1 shows the atomic percentage of all the elements present in the samples.

Following with the luminescence characterization, the emission spectra of all the samples were measured using selective excitations at 379 nm and 409 nm, that correspond to the energy levels of $^4G_{11/2}$, and $^2H_{9/2}$, respectively. Fig. 3 shows emission

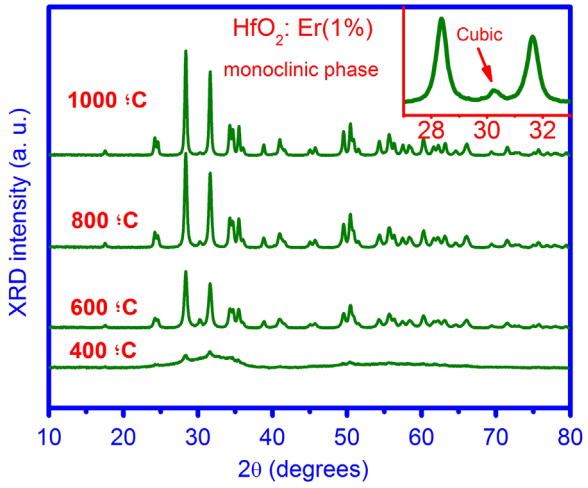

Fig. 2. X-ray diffraction plots for HfO_2:Er samples for all sinterization temperatures. The inset shows a diffraction peak that does not correspond to the monoclinic phase.

Table 1
Atomic percentage of oxygen, hafnium, erbium and chlorine in HfO_2:Er^{+3} samples for all different sinterization temperatures.

Sinterization temperature [°C]	Oxygen [%]	Hafnium [%]	Erbium [%]	Chlorine [%]
400	65.79	30.55	0.92	2.74
600	66.75	30.73	0.84	1.68
800	66.28	32.21	0.70	0.81
1000	66.79	32.45	0.65	0.11

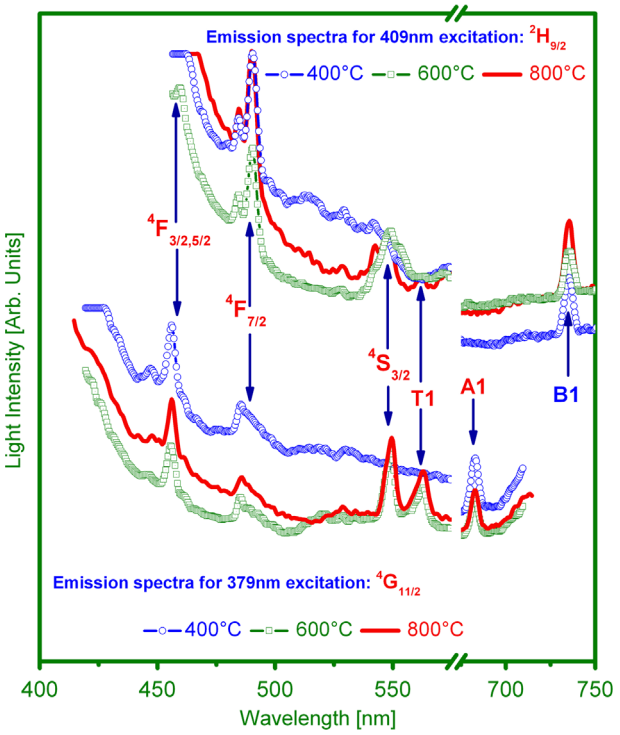

Fig. 3. Emission spectra for HfO_2:Er^{3+} samples. The upper set of plots represents the emission spectra for an excitation wavelength of 409 nm and the lower set is formed by an excitation of 379 nm.

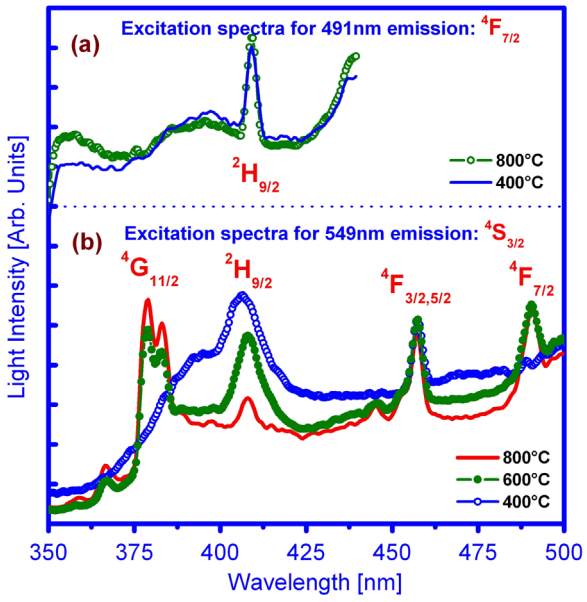

Fig. 4. Excitation spectra of HfO_2:Er^{3+} samples for a series of different sinterization temperatures. (a) Excitation spectra for an emission at 491 nm for the sinterization temperature of 400 °C and 800 °C. (b) Excitation spectra for an emission at 549 nm for 400 °C, 600 °C and 800 °C. All the corresponding energy levels shown by the excitation spectra are properly identified and labeled.

spectra for sinterization temperatures of 400 °C, 600 °C and 800 °C. The lower set of three plots are emission spectra that correspond to an excitation wavelength of 379 nm while the upper set results from an excitation at 409 nm. The emission intensity vs. wavelength plots are labeled using the same distinctive lines for similar temperatures in both sets. In addition to the characteristic emission wavelengths of the Er ion at 459 nm, 490 nm, and 549 nm, labeled in both sets with the corresponding energy level, three additional emission peaks are labeled with the tags T1, A1 and B1. The corresponding wavelengths for these transitions are 563 nm, 683 nm and 735 nm.

Some important points can be addressed from Fig. 3: (1) typical emissions stimulated by transitions to the ground state or to other excited multiplet states can be identified. Emission wavelengths at 459 nm, 491 nm, and 549 nm that correspond to transitions from the states $^4F_{3/2,\ 5/2,\ 7/2}$ and $^4S_{3/2}$ to the ground state $^4I_{15/2}$, and 563 nm, 683 nm and 735 nm which correspond to the transitions $^2H_{9/2}$ to $^4I_{13/2}$, $^2H_{9/2}$ to $^4I_{11/2}$ and $^4F_{7/2}$ to $^4I_{13/2}$ respectively, confirm the activation of Er ions in HfO_2 matrix. (2) It is clear from Fig. 3 that for sinterization temperatures below 600 °C, the condition for emissions at 549 nm and 563 nm are not yet formed in the samples. (3) Emission A1 is not present for spectra excited with 409 nm and B1 does not appear in spectra excited with 379 nm and (4) the dominant transition when exciting at 379 nm is the $^4S_{3/2}$ to $^4I_{15/2}$ ground state and for the excitation at 409 nm is from $^4F_{7/2}$ to $^4I_{15/2}$.

Based on the facts addressed above, we infer the importance of analyzing the excitation spectra for the emission of the two dominant transitions in Fig. 3. The aim is to understand why the transition $^4S_{3/2}$ to $^4I_{15/2}$ is not formed for sinterization temperatures below 600 °C. Fig. 4 shows the excitation spectra of the HfO_2:Er^{3+} samples for two emission wavelengths, (a) emission at 491 nm ($^4F_{7/2}$ to $^4I_{15/2}$) for samples treated at 400 °C and 800 °C and (b) emission at 549 nm ($^4S_{3/2}$ to $^4I_{15/2}$) for samples treated at 400 °C, 600 °C, and 800 °C. In both parts of the figure the excitation peaks have been identified with the corresponding levels of the multiplet state and all the spectra have been plotted with the same distinctive lines for the similar sinterization temperatures.

Analyzing the Fig. 4(a), it is possible to observe that the transition from $^4F_{7/2}$ multiplet to the ground state comes from the energy level $^2H_{9/2}$, and that this transition does not depend on the sinterization temperatures at least for the emission at 491 nm, which gives us a feeling of steady behavior. However, if we look at Fig. 4(b) we can observe some important facts. (1) For samples treated at 400 °C the excitation spectrum does not show any contribution from $^4G_{11/2}$ but shows a very intense contribution from $^2H_{9/2}$, in contrast with the rest of the sinterization temperatures. It is also clear that the $^4F_{7/2}$ does not take part in the emission at 549 nm either. (2) We observe that as the sinterization temperature increases the conditions for the contribution from $^4G_{11/2}$ improve and this transition becomes dominant while the contribution from $^2H_{9/2}$ decreases notably, the ones from $^4F_{3/2,\ 5/2}$ stay steady and the one from $^4F_{7/2}$ appears and remains stable.

The behavior addressed here and the important points mentioned in both figures describe the effects of sinterization temperature on photoluminescence of the HfO_2:Er^{3+} samples and might be explained with a dual lattice site occupation of the Er during its incorporation to the HfO_2 matrix. In order to show in a cleaner way the difference detected in the luminescent behavior of the HfO_2:Er^{3+} samples, we introduce an energy level diagram. Fig. 5 shows the calculated energy levels for free Er^{3+} ion and a comparison of the two observed emission behaviors of the HfO_2:Er^{3+} samples. The left part of the figure shows the energy axis in 1/cm units together with the free Er ion energy levels. The two configurations detected are indicated by showing with solid upward arrows the initial excitation wavelength at 379 nm for configuration A and at 409 nm for configuration B. The two solid downward arrows show the dominant transitions for both configurations, a transition from $^4S_{3/2}$ to $^4I_{15/2}$ for configuration A and from $^4F_{7/2}$ to $^4I_{15/2}$ for configuration B, and finally the two dashed line arrows denote the two particular transitions exclusively shown by each configuration, A1 and B1. Configuration B1 might

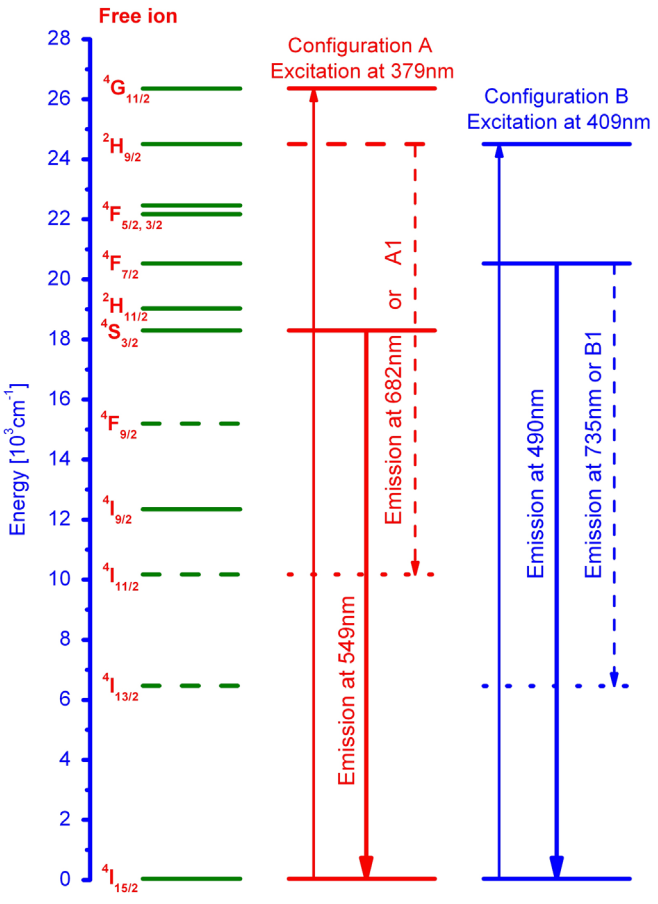

Fig. 5. Energy levels for the free erbium ion calculated using the intermediate coupling theory and a comparison of the two observed emission configurations.

be related to the structure associated with the small diffraction peak shown in the Fig. 2 inset, since the emission spectra also appears at 490 nm.

In summary, we investigated the sinterization temperature effects on the photoluminescence properties of Er-doped HfO_2 samples giving the observed emission and excitation spectra for different excitation/emission wavelengths. Standard and special transitions, as well as two configurations of the Er in the HfO_2 matrix were observed and analyzed at different temperatures. The existence of a threshold sinterization temperature was observed that allows the strong excitation at the $^4G_{11/2}$ energy level and its respective emission in green at 549 nm. This transition does not even appear when the sinterization temperature is lower than 600 °C (Figs. 3 and 4). The erbium occupation of two different sites within the HfO_2 matrix is demonstrated with the observation of two different dominant emissions at 490 nm (configuration B) and 549 nm (configuration A) together with the presence of special transitions A1 and B1 with emissions at 682 nm and 735 nm, respectively.

As a result, it is possible to conclude that HfO_2 matrix represents a good host to contain the Er^{3+} ions, taking into account that for temperatures above 600 °C the crystal size allows the incorporation of more Er^{3+} ions resulting in a much more effective excitation/emission process. Moreover, the HfO_2 matrix allows for some tailoring of the excitation/emission wavelengths by changing the sinterization temperature, making it possible to enhance emissions in the blue-green and green and red regions.

Acknowledgment

This work was supported by PAPIIT, UNAM under Project IN102510.

References

[1] A. Polman, J. Appl. Phys. 82 (1997) 1.
[2] A.J. Kenyon, Semicond. Sci. Technol. 20 (2005) R65.
[3] S. Ossicini, L. Pavesi, F. Priolo, Light Emitting Silicom for Microphotonics, Springer, Berlin (2003) 179(Chapter 5).
[4] J.Z. Wang, Z.Q. Shi, Y. Shi, L. Pu, L.J. Pan, R. Zhang, Y.D. Zheng, Z.S. Tao, F. Lu, Appl. Phys. A 94 (2009) 399.
[5] R. Serna, M. Jimenez de Castro, J.A. Chaos, A. Suarez-Garcia, C.N. Afonso, M. Fernandez, I. Vickridge, J. Appl. Phys. 90 (2001) 5120.
[6] J. Hoang, T.T. Van, M. Sawkar-Mathur, B. Hoex, M.C.M. Van de Sanden, W.M.M. Kessels, R. Ostroumov, K.L. Wang, J.R. Bargar, J.P. Changa, J. Appl. Phys. 101 (2007) 123116.
[7] J.L. Bubendorff, J. Ebothé, A. El Hichou, R. Dounia, M. Addou, J. Appl. Phys. 100 (2006) 014505.
[8] M. Miritello, R.L. Savio, F. Iacona, G. Franzò, A. Irrera, A.M. Piro, C. Bongiorno, F. Priolo, Adv. Mater. 19 (2007) 1582.
[9] A. Polman, F.C.J.M. van Veggel, J. Opt. Soc. Am. B 21 (2004) 871.
[10] M.L. Gong, J.X. Shi, W.K. Wong, K.K. Shiu, W.H. Zheng, K.W. Cheah, Appl. Phys. A 68 (1999) 107.
[11] C. Ugolini, N. Nepal, J.Y. Lin, H.X. Jiang, J.M. Zavada, Appl. Phys. Lett. 90 (2007) 051110.
[12] L.D. da Vila, L. Gomes, L.V.G. Tarelho, S.J.L. Ribeiro, Y. Messadeq, J. Appl. Phys. 93 (2003) 3873.
[13] N. Managaki, M. Fujii, T. Nakamura, Y. Usui, S. Hayashi, Appl. Phys. Lett. 88 (2006) 042101.
[14] A. Martucci, M. de Nuntis, A. Ribaudo, M. Guglielmi, S. Padovani, F. Enrichi, G. Mattei, P. Mazzoldi, C. Sada, E. Trave, G. Battaglin, F. Gonella, E. Borsella, M. Falconieri, M. Patrini, J. Fick, Appl. Phys. A 80 (2005) 557.
[15] S. Gallis, M. Huang, A.E. Kaloyeros, Appl. Phys. Lett. 90 (2007) 161914.
[16] S. Kim, S.J. Rhee, D.A. Turnbull, X. Li, J.J. Coleman, S.G. Bishop, P.B. Klein, Appl. Phys. Lett. 71 (1997) 2662.
[17] L.F. Bian, C.G. Zhang, W.D. Chen, C.C. Hsu, T.F. Shi, Appl. Phys. Lett. 89 (2006) 231927.
[18] N.E. Byer, T.C. Ensigh, W.M. Mularie, S.E. Stokowski, J. Appl. Phys 44 (1973) 1733.
[19] G.N. van den Hoven, A. Polman, E. Alves, M.F. da Silva, A.A Melo, J. Mater. Res. 12 (1997) 1401.
[20] Junzhuan Wang, Yan Xia, Yi Shi, Zhuoqiong shi, Lin Pu, Rong Zhang, Youdou Zheng, Zhensheng Tao, Fang Lu, Appl. Phys. Lett. 91 (2007) 191115.
[21] S. Hüfner, Optical Spectra of Transparent Rare Earth Compounds, Academic Press, Inc., New York, 1978.